

# Ground-Motion Attenuation in the Atlantic Coastal Plain near Charleston, South Carolina

by Martin C. Chapman, Pradeep Talwani, and Richard C. Cannon

**Abstract** Charleston, South Carolina, lies on approximately 1 km of Cretaceous and Cenozoic sediments of the Atlantic Coastal Plain. Estimation of high-frequency absorption due to these sediments is important for strong motion prediction. We attempt the measurement using microearthquake data recorded at small distances by surface and shallow subsurface short-period stations in the Middleton Place—Summerville seismic zone. The problem is difficult because it involves potential bias due to the seismic source, propagation through basement, and strong site-specific spectral modulation. Previous studies involving drilling and seismic reflection profiling indicate a 775-m thickness of sediments, with average vertical  $P$ - and  $S$ -wave velocities of 2.14 and 0.700 km/sec for the network area. The attenuation parameter  $\kappa$  ( $\kappa_s$  and  $\kappa_p$ ) for  $S$  and  $P$  waves is estimated from spectral analysis of the direct  $S$  and converted  $Sp$  phases. The ratio of  $S$  to  $Sp$  provides a useful check for bias. Multiple linear regression using all stations yields  $\kappa_s = 0.049$  and  $\kappa_p = 0.024$ . The regression results are interpreted as upper-bound estimates because they assume source corner frequencies in excess of 25 Hz. A similar analysis is carried out for a hard-rock environment using reservoir-induced microearthquakes at Lake Monticello, South Carolina. From that, we estimate a maximum potential bias of  $0.014 \text{ sec}^{-1}$ , yielding  $0.035 < \kappa_s < 0.049$  and  $0.010 < \kappa_p < 0.024$  as likely values near Charleston. We favor the lower limits of these ranges because they imply numerically similar values for the path-average quality factors ( $Q_s = 32$ ,  $Q_p = 36$ ), whereas the upper range values imply that  $Q_s$  is substantially larger than  $Q_p$  ( $Q_s = 22$ ,  $Q_p = 15$ ).

## Introduction

Charleston, South Carolina, experienced an earthquake on 31 August 1886 with an estimated magnitude in excess of 7.0 (Johnston, 1996). Paleoseismic investigations suggest seven episodes of prehistoric liquefaction in the past 6000 years in the lower coastal plain of South Carolina (Talwani and Schaeffer, 2001). The population of the Charleston area is increasing and is exposed to the highest level of seismic hazard along the eastern seaboard of the United States (Frankel *et al.*, 2002). Ground-motion prediction is complicated by the geological conditions. Approximately 1000 m of weakly consolidated Cretaceous and Cenozoic sediment overlies high-velocity basement rock in this area. The shallow materials at many locations are Quaternary beach and barrier island deposits with very low seismic velocities. These deposits exhibited nonlinear behavior, including liquefaction, under strong shaking in 1886.

This study focuses on quantifying the attenuation of weak motions in the Atlantic Coastal Plain sedimentary sequence near Charleston for purposes of strong ground motion prediction. Appreciable anelastic absorption of these materials will have an effect on high-frequency ground-

motion levels. Accurate assessment of absorption within the bulk of the sedimentary sequence is necessary for modeling the potential nonlinear behavior of shallower materials. Insofar as peak acceleration remains the primary quantifying parameter for shaking intensity in building codes and in many earthquake-resistant design procedures, accurate quantification of high-frequency attenuation is an important issue for Charleston and other urban areas in similar geological settings in the eastern United States.

Previous measurements of attenuation in the area include the work of Rhea (1984) and Fletcher (1995). Rhea (1984) used stations in the Charleston area to estimate coda  $Q$ . The coda contains a complex of scattered surface and body waves, involving the upper crust including the shallow coastal plain section. Her estimates of coda  $Q$  are significantly lower than coda  $Q$  estimates determined in areas of eastern North America where hard rock is exposed at the surface. This suggests that attenuation in the sedimentary section is appreciable. Fletcher (1995) primarily used data recorded at the Savannah River site near Aiken, South Carolina, in the coastal plain approximately 140 km to the west

of Charleston. His study focused on determination of earthquake source parameters and crustal  $Q$  values.

In this study, direct phase arrivals from microearthquakes recorded at small distances will be used to measure attenuation near Charleston. The study takes advantage of simple earthquake sources and short ray-path lengths. These conditions reduce bias due to source spectral shape and attenuation in the basement part of the path. Some information on the degree of possible bias is provided by analysis of data from reservoir-induced microearthquakes recorded at small distances near Lake Monticello, South Carolina, in a low-attenuation, hard-rock environment.

### Data and Background

Figure 1 shows the two areas of interest in this study. The objective is to derive estimates of attenuation for the coastal area near Charleston. In doing so, data from a three-component station near Monticello reservoir in central South Carolina will be used for comparison with results obtained in the coastal area. Lake Monticello is an impoundment situated on hard Paleozoic crystalline rock. The reservoir-induced seismicity there occurs at very shallow depth (Chen and Talwani, 2001).

The data are three-component recordings from the University of South Carolina network. Figure 2 shows the locations of the three-component stations WAS, RGR, CSU, and CSB, as well as the epicenters of 25 earthquakes that provided the data selected for analysis in the coastal area near Charleston. Table 1 lists the hypocenter parameters and magnitudes of these earthquakes. Figure 3 shows the location of station JSC near Lake Monticello and the 23 earthquakes that provided additional data. Table 2 lists the hypocenters and magnitudes of the Lake Monticello earthquakes.

The recording stations use short-period sensors. Stations RGR and CSB are installed in backfilled boreholes at depths of 62 and 83 m, respectively, and both incorporate 4-Hz sensor packages. The surface stations WAS, CSU, and JSC near Lake Monticello use 1-Hz sensors. CSU and CSB are colocated. Analog data from the stations are telemetered to the central recording facility, sampled at a rate of  $100 \text{ sec}^{-1}$ , and recorded in event-triggered mode.

Earthquakes in coastal South Carolina are associated with the Middleton Place–Summerville seismic zone, in the epicentral tract of the major 31 August 1886 earthquake (Fig. 2). The seismicity has been instrumentally monitored since 1975. Most of the earthquakes define a dense cluster that has been interpreted to represent an intersection of basement faults: a southwest-dipping reverse fault trending northwest parallel to the Ashley River and a northeast-striking, near-vertical strike-slip fault (Talwani 1982; Madabhushi and Talwani 1993; Talwani 1999). The seismicity involves the upper crust, to a depth of approximately 15 km.

The shallow crustal velocity structure near Charleston is understood primarily as a result of investigations per-

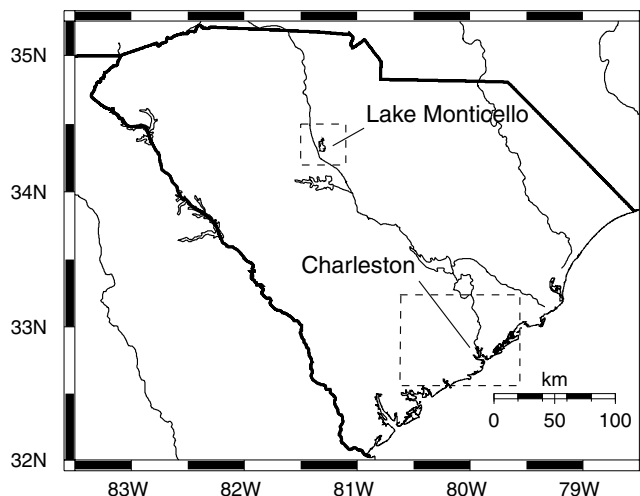


Figure 1. The rectangles show the locations of the study areas near Charleston and Lake Monticello in South Carolina.

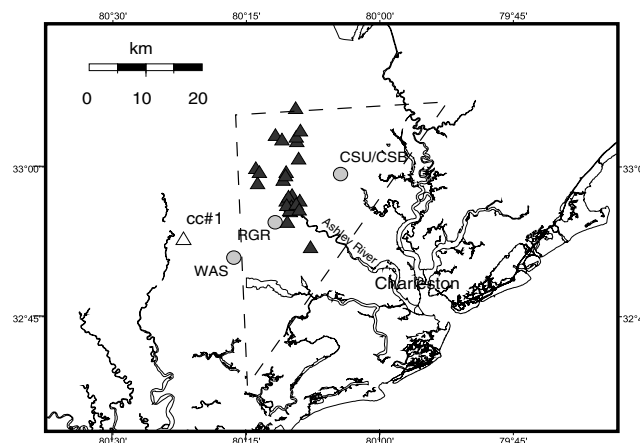


Figure 2. The study area near Charleston, South Carolina (shown as the larger rectangle in Fig. 1). Filled triangles indicate earthquake epicenters in the Middleton Place–Summerville seismic zone. Seismic stations are shown by filled circles. Stations CSB and RGR are in boreholes at 83 and 62 m depth, respectively. The open triangle indicates the location of Clubhouse Crossroads well number 1. The dashed triangle is a generalized interpretation of the epicentral area of the 1886 shock, from the isoseismal map of Dutton (1889).

formed during the decade 1973–1983 (see Rankin [1977] and Gohn [1983] for summaries). Of particular relevance to the present study is the sonic log from Clubhouse Crossroads well number 1 (cc1; “cc#1” in Fig. 2) and nearby vertical incidence reflection and refraction profiles (Ackerman 1983; Yantis *et al.*, 1983). A strong seismic reflector corresponding to the top of an early Jurassic basalt layer marks the top of the basement beneath the recording sites. This basalt was encountered at a depth of 775 m in the cc1 well. Interval  $P$ -

Table 1  
Listing of Earthquakes Near Charleston Used for Analysis

Date (yy/mm/dd)	Day No.	Hr:Mn:Sec	Latitude (°N)	Longitude (°W)	Depth (km)	Magnitude
98/02/06	(037)	01:09:47.7	32.9247	80.1670	5.6	0.9
98/03/29	(088)	20:36:52.0	32.9398	80.1487	9.4	1.7
98/05/04	(124)	21:44:08.6	32.9323	80.1733	10.5	2.2
98/07/19	(200)	15:02:46.59	32.9948	80.2308	11.7	1.8
98/09/11	(254)	03:52:57.4	33.0942	80.1560	9.9	2.1
98/10/31	(304)	01:24:29.7	33.0495	80.1937	8.7	1.8
98/11/05	(309)	19:47:45.4	32.9342	80.1552	5.7	1.5
98/11/11	(315)	07:42:35.6	32.9823	80.1755	7.3	1.3
98/11/13	(317)	02:14:59.1	32.9882	80.2238	12.5	2.0
98/11/15	(319)	18:48:06.4	33.0472	80.1552	8.86	2.1
99/03/29	(088)	16:43:07.8	33.0572	80.1468	7.9	2.0
99/07/24	(205)	22:45:50.7	32.9248	80.1500	5.1	1.2
99/09/27	(270)	04:03:53.2	33.0425	80.1815	10.1	1.6
00/01/11	(011)	10:03:20.1	32.8620	80.1298	2.5	0.8
00/05/21	(142)	02:39:05.4	32.9403	80.1740	7.8	1.8
00/09/04	(248)	07:36:20.4	32.9227	80.1657	6.3	1.3
00/09/22	(266)	04:25:16.5	33.0010	80.1507	4.8	2.4
00/10/19	(293)	18:12:45.7	32.9685	80.2272	12.3	2.0
01/02/04	(035)	03:34:12.0	32.9470	80.1690	6.4	1.6
01/02/11	(042)	10:31:34.8	32.9753	80.1795	7.6	1.3
01/03/08	(067)	07:34:26.3	32.9248	80.1602	11.4	1.7
01/03/11	(070)	11:32:06.7	33.0395	80.1543	6.15	2.4
01/03/24	(083)	06:02:39.6	32.9050	80.1722	9.4	1.4
01/04/15	(105)	19:43:38.2	32.9877	80.1737	7.7	1.3
01/04/28	(118)	07:27:43.3	32.9313	80.1638	2.1	2.1

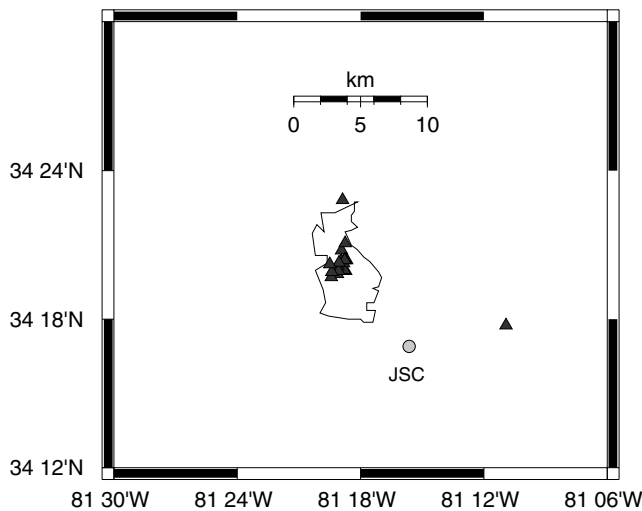


Figure 3. The study area near Lake Monticello, shown as the small rectangle in Figure 1. The thin line shows the approximate shoreline of the reservoir. The filled triangles indicate reservoir-induced earthquake epicenters. Three-component station JSC is shown by the filled circle.

wave seismic velocities in the overlying sediments are variable (Fig. 4), but generally lie in the range 1.8–2.6 km/sec.

The  $P$ -wave vertical travel time through the sedimentary sequence at cc1 is accurately determined from the observed two-way time of 0.725 sec for the top of the basalt reflector

at that location (Yantis *et al.*, 1983). Given a thickness of 775 m of sediments at cc1, this gives an average velocity of 2.14 km/sec for vertical  $P$ -wave propagation through the Cretaceous–Cenozoic sedimentary section. Refraction profiling (Ackerman 1983) indicates that the sedimentary sequence thickens to the east and southeast from the cc1 well. The contour map of Ackerman (1983) suggests a 1000-m thickness of sediments beneath the city of Charleston.

Figures 5 and 6 show seismograms from the four recording stations near Charleston. The impedance contrast at the base of the sedimentary sequence generates a strong  $S$  to  $P$  ( $S_p$ ) phase conversion, which is the most prominent arrival on the vertical component. The  $S_p$  and the  $P$  to  $S$  ( $P_s$ ) converted phases are observed in thick sedimentary basins and coastal plain environments featuring high-velocity basement rock. Examples from the Gazli, Uzbekistan, and Mississippi Embayment areas were discussed by Clouser and Langston (1991) and Chen *et al.* (1994), respectively. In this study area, the  $S_p$  phase arrives on average 0.74 sec prior to the direct  $S$  wave on the transverse component at CSU and WAS (Garner, 1998). This arrival-time interval, along with the observed vertical  $P$ -wave travel time of 0.363 sec on reflection profiles near cc1, implies that the average vertical  $S$ -wave travel time through the sediments is 1.10 sec and that the average  $P/S$  velocity ratio is 3.04. Figure 4 shows a simplified layered  $P$ - and  $S$ -wave velocity model, which assumes a constant  $P/S$  velocity ratio throughout the sedimentary sequence. The  $P$ -wave velocities of the sedimentary lay-

Table 2  
Listing of Earthquakes Near Lake Monticello Used for Analysis

Date (yy/mm/dd)	Day No.	Hr:Min:Sec	Latitude (°N)	Longitude (°W)	Depth (km)	Magnitude
00/01/05	(005)	21:06:37.6	34.3462	81.3153	0.5	0.9
00/04/17	(108)	07:18:40.4	34.3510	81.3125	2.1	0.3
00/06/04	(156)	12:13:31.6	34.3303	81.3187	1.0	0.4
00/06/09	(161)	11:36:41.4	34.3325	81.3122	1.6	0.7
00/06/16	(168)	13:12:13.7	34.3330	81.3180	1.2	1.1
00/06/18	(170)	01:51:48.0	34.3348	81.3158	0.1	1.0
00/06/24	(176)	17:04:01.0	34.3333	81.3132	0.4	0.9
00/07/01	(183)	02:00:42.3	34.3357	81.3183	0.2	1.0
00/07/04	(186)	15:56:48.2	34.3368	81.3250	1.6	0.2
00/07/29	(211)	07:41:43.6	34.1949	81.3238	1.1	0.7
00/08/27	(240)	21:30:26.9	34.3282	81.3237	1.4	1.2
00/09/13	(257)	19:04:20.7	34.3802	81.3147	2.4	1.2
00/09/29	(273)	16:20:47.4	34.3317	81.3232	0.2	1.1
00/10/22	(296)	05:32:02.0	34.2957	81.1822	1.2	0.4
00/11/03	(308)	07:34:48.7	34.3385	81.3155	0.9	1.0
00/11/04	(309)	00:54:39.4	34.3380	81.3174	0.5	0.1
00/11/05	(310)	08:53:49.7	34.3397	81.3130	0.9	0.4
00/11/07	(312)	09:58:40.5	34.3398	81.3122	0.8	0.4
00/11/08	(313)	00:15:53.0	34.3397	81.3113	0.7	0.3
00/11/15	(320)	08:48:04.5	34.3323	81.3178	1.1	0.1
00/11/17	(322)	00:20:16.1	34.3390	81.3157	1.4	0.4
00/11/17	(322)	00:35:53.4	34.3410	81.3130	0.7	0.5
00/11/20	(325)	04:22:01.1	34.3376	81.3138	0.8	0.1

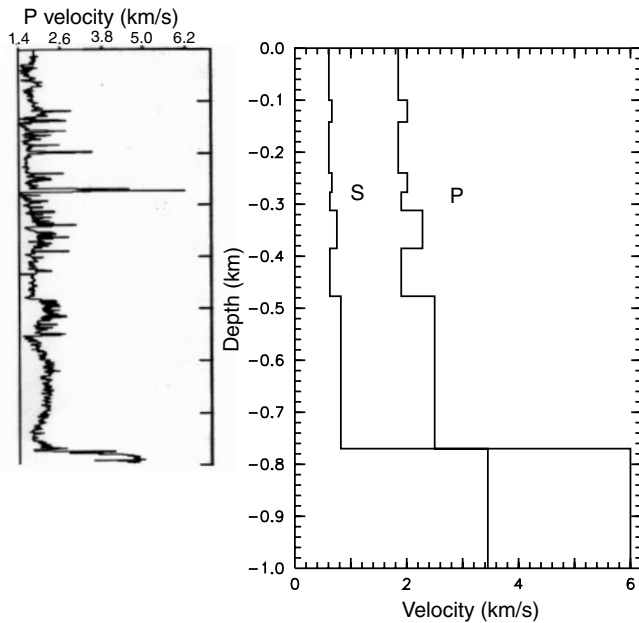


Figure 4. Left:  $P$ -wave velocity log from Clubhouse Crossroads well number 1 (from Yantis *et al.*, 1983). Right: Interpreted layered velocity structure.

ers were adjusted to yield a vertical travel time of 0.363 sec, as observed on nearby reflection profiles.

Figure 7 shows seismograms from station JSC near Lake Monticello. The seismicity associated with the reservoir is typically at depths of less than 2.0 km. The reservoir is located in a complex metamorphic terrane intruded by plutons

of granite and granodiorite composition (Chen and Talwani, 2001). Although the ray paths from the hypocenters to station JSC are at shallow depth, the high velocity of the near-surface rock implies minimal attenuation.

### Analysis

We assume the following model for the  $S$ -wave acceleration amplitude spectrum in the Charleston area:

$$A_s(f) = \text{Source}_s(f) \text{Path}_s^{\text{base}}(f) \text{Path}_s^{\text{sed}}(f). \quad (1)$$

The terms on the right side of equation (1) represent the earthquake source spectrum, the effects of propagation through the basement, and the propagation through the sedimentary section, respectively. The last term on the right in equation (1) can be considered the “site” response. The path effect is modeled using only the basement term for the Lake Monticello data, because the recording station is sited on hard rock. Using the attenuation parameterization of Anderson and Hough (1984), we assume that the total path attenuation is represented by a distance-dependent element, related to ray paths within the basement, and, in the case of the Charleston data, a distance-independent element due to attenuation in the sediments under the recording site. Hence, for a given site near Charleston,

$$A_s = \text{Source}_s \Phi_s^{\text{base}} \exp(-\pi\kappa_s^{\text{base}} f) \Phi_s^{\text{sed}} \exp(-\pi\kappa_s^{\text{sed}} f). \quad (2)$$

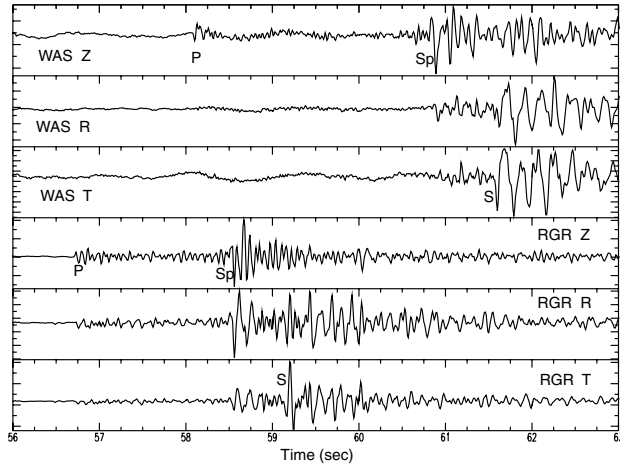


Figure 5. Vertical (Z), radial (R), and transverse (T) component recordings from stations WAS (top) and RGR (bottom) for the  $M = 1.6$ , 27 September 1999 earthquake. Epicentral distances are 23 and 15 km, respectively, and the depth was 10 km.  $P$ -,  $Sp$ -, and  $S$ -wave arrivals are indicated. RGR is at a depth of 62 m.

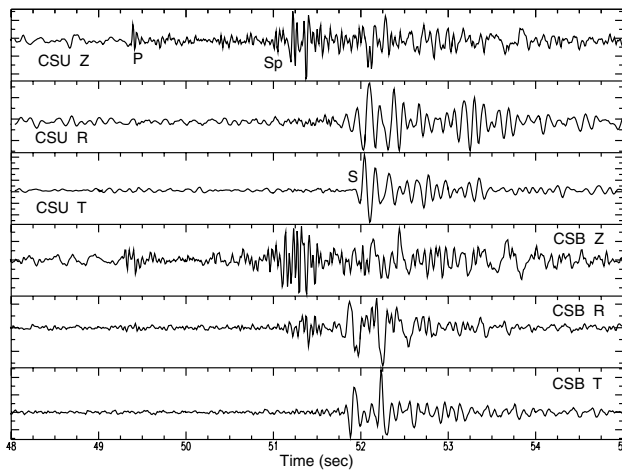


Figure 6. Vertical (Z), radial (R), and transverse (T) component recordings from collocated stations CSU (top) and CSB (bottom) for the  $M = 2.0$ , 19 October 2000 earthquake. The epicentral distance is 14.8 km, and the depth was 12 km.  $P$ -,  $Sp$ -, and  $S$ -wave arrivals are indicated. Note that CSB is at a depth of 83 m, therefore showing earlier arrival times and reflections from the free surface.

In the absence of frequency-dependent attenuation, the parameter “kappa” for  $S$  waves  $\kappa_s$  is related to the quality factor  $Q$  through

$$\kappa_s = \int \frac{ds}{Q(s)\beta(s)}. \quad (3)$$

In equation (3),  $\beta$  is the shear-wave velocity and the integral is along the ray path.

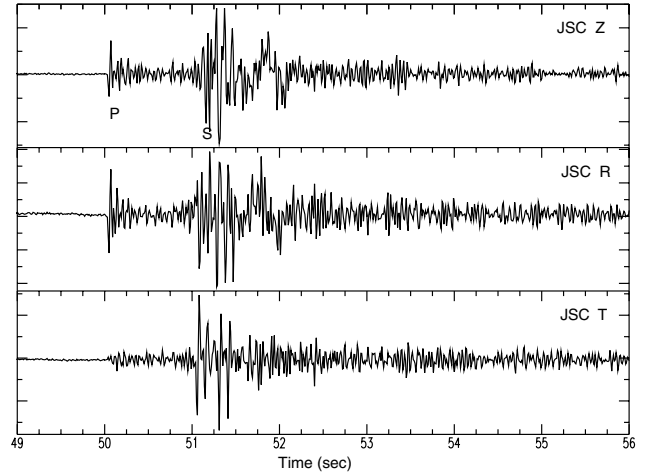


Figure 7. Vertical (Z), radial (R), and transverse (T) component recordings from station JSC for the  $M = 1.0$ , 11 November 2000 earthquake at Lake Monticello. The epicentral distance is 8.3 km, and depth was 0.9 km. Note the prominent Rayleigh wave on the vertical and radial components and the higher frequency content of the  $S$  wave compared to Figures 5 and 6.

We assume a uniform half-space velocity model beneath the coastal plain section:  $\Phi_s$  for this basement portion of the ray path is independent of frequency and simply represents geometrical spreading. The term  $\Phi_s$  for the sedimentary section represents the frequency-dependent effects of propagation within the plane layered sequence and involves scattering and interference:  $\Phi_s$  of the sediments thus represents site response without absorption.

Studies of coda-wave and  $Lg$  attenuation at regional distances in the Appalachians generally indicate low loss. For example, Chapman and Rogers (1989) found  $Q = 811f^{0.42}$  for the frequency range 1–12 Hz from analysis of coda waves for paths in the southern Appalachian highlands. Benz *et al.* (1997) found  $Q = 1052f^{0.22}$  for the frequency range 1–14 Hz in the northeastern United States and southeastern Canada, results that are representative of several other studies of attenuation in that region. On the basis of these regional studies, it appears that a representative value for shear-wave  $Q$  is at least 1600 for frequencies greater than 10 Hz in the upper crustal rocks of the Appalachians. The maximum source–receiver distance in this study is less than 30 km. Using that value and assuming that the shear-wave  $Q$  is 1600 with a basement shear-wave velocity of 3.45 km/sec gives  $\kappa_s = 0.006$  for that part of the path. Loss of that magnitude is not resolvable in this data set. Given these considerations, and assuming an  $\omega^2$  source spectrum, we rewrite equation (2) for the Charleston area as

$$A_s = C \frac{(2\pi f)^2}{1 + (f/f_c)^2} \Phi_s^{\text{sed}} \exp(-\pi\kappa_s^{\text{sed}} f). \quad (4)$$

The constant  $C$  incorporates geometrical spreading, seismic moment, radiation pattern, and material properties of the source region. The corner frequency of the source spectrum is represented by  $f_c$ .

Determination of  $\kappa_s$  near Charleston is problematic because it requires isolating or otherwise accounting for the effects of source spectrum corner frequency  $f_c$  and site response  $\Phi_s$ . Ideally, these difficulties could be handled with data from a deep borehole vertical array. Such data do not exist currently for the Charleston area, and we cannot be sure that the earthquake source and site response do not bias the results we derive here using a distributed network of surface and shallow subsurface stations. However, we hope to assess the nature and possible degree of bias.

The Charleston area data are from microearthquakes with magnitudes less than 2.5. We assume that  $f_c > 25$  Hz for all events, as a working hypothesis. If in fact the corner frequencies are significantly lower, the analysis procedure described below will overestimate  $\kappa$ . Examination of the data shows that  $\Phi_s$  is strongly modulated in the frequency band 1–10 Hz, particularly for the surface stations WAS and CSU. These amplifications are due to shallow site conditions. We hope to at least partially overcome this problem by combining the data from all four stations in a joint estimation, which will tend to randomize these site-specific effects. Also, the coherent peaks in the individual site spectra are less prominent at frequencies greater than approximately 10 Hz. The spectra appear approximately random at the higher frequencies, when all spectra for a given station are examined in composite. This suggests that  $\Phi_s$  at frequencies greater than 10 Hz may be modeled as a white noise spectrum as a crude approximation. For example, we can model the site response as  $\ln \Phi_s = E(\ln \Phi_s) + \varepsilon_s$ , where  $E(\ln \Phi_s)$  is the (constant) mean logarithm of the shear-wave site response and  $\varepsilon_s$  is a normally distributed random variable with zero mean that represents the random component. With these assumptions, we represent the log amplitude spectrum as

$$\ln \frac{A_s}{(2\pi f)^2} = b_s - \pi \kappa_s f + \varepsilon_s, \quad (5)$$

where  $\kappa_s$  refers exclusively to shear-wave loss in the sediments and the intercept  $b_s = \ln C + E(\ln \Phi_s)$  is assumed constant for a given recorded amplitude spectrum. The slope of this relationship estimated by linear regression gives an estimate of the attenuation parameter  $\kappa_s$ .

The model expressed by equation (5) involves strong assumptions regarding the statistical nature of the site response, as well as the source spectrum corner frequency. It is impossible to fully test these assumptions with the available data. However, a weak test is possible by forming the spectral ratio of the direct shear wave and the converted  $Sp$  arrival to estimate the difference  $\kappa_s - \kappa_p$  (Clouser and Langston, 1991). The effects of the source spectrum are cancelled in forming the  $Sp/S$  ratio. The approach we will use here is

to independently estimate  $\kappa_s$  from the direct shear wave on the transverse components and  $\kappa_p$  from the  $Sp$  arrival on the vertical components. The difference of these two direct estimates can then be compared with an estimate of  $\kappa_s - \kappa_p$  from the spectral ratio of the  $S$  and  $Sp$  phases. The comparison also involves different site response functions  $\Phi_s$  and  $\Phi_p$  and the ratio  $\Phi_s/\Phi_p$ . Close agreement between the estimate of  $\kappa_s - \kappa_p$  derived from the spectral ratios and the direct phases would suggest that the assumptions concerning the source spectra are viable, and that  $\Phi_s$ ,  $\Phi_p$ , and  $\Phi_s/\Phi_p$  are approximated by white noise, thereby lending some confidence that the estimates of  $\kappa_s$  and  $\kappa_p$  are not strongly biased.

The amplitude spectrum for the  $Sp$  converted arrival is, in analogy to equation 5,

$$\ln \frac{A_{sp}}{(2\pi f)^2} = b_p - \pi \kappa_p f + \varepsilon_p. \quad (6)$$

For the spectral ratio, we have

$$\ln(A_s/A_{sp}) = b' - \pi (\kappa_s - \kappa_p) f + \varepsilon', \quad (7)$$

where  $b' = E(\ln \Phi_s) - E(\ln \Phi_p)$  is assumed constant over the frequency band of interest and  $\varepsilon' = \varepsilon_s - \varepsilon_p$  is normally distributed with zero mean. The multiple linear regression model used to estimate  $\kappa_s$ ,  $\kappa_p$ , and  $\kappa_s - \kappa_p$  is of the form

$$\ln(Y^i) = \sum_{j=1}^n b_j G_j - \alpha \pi f. \quad (8)$$

In the above,  $Y^i$  represents the observed displacement amplitude ordinate or ratio, at frequency  $f$ , for the  $i$ th spectrum,  $i = 1, 2, \dots, n$ , where  $n$  is the total number of spectra or spectral ratios from all four stations combined. Note that  $G_j = 1$  if  $i = j$ ,  $G_j = 0$  otherwise. The simultaneous least-squares solution for the  $n + 1$  unknowns gives a joint estimate of  $\kappa_s$ ,  $\kappa_p$ , or  $\kappa_s - \kappa_p$  and individual estimates of  $b_s$ ,  $b_p$ , or  $b'$  for each spectrum or spectral ratio.

#### Lake Monticello $\kappa_s$ Estimation

Because of the weak attenuation at this hard-rock site, the data from Lake Monticello provide some insight into the potential effects of the source spectrum on the estimation of  $\kappa$  from the Charleston area data.

The JSC data were corrected for instrument response and rotated into radial and transverse components. The acceleration Fourier amplitude spectrum of the  $S$ -wave arrival on the transverse component was computed using a 0.5 sec processing window. The window incorporated a 10% cosine taper at the end. The windowed time series were padded to 128 points (sample rate 100 sec<sup>-1</sup>). The resulting spectra were smoothed using a three-point moving average.

An accurate assessment of the signal-to-noise ratio for each spectrum is important. The pre- $S$  portions of the seismograms were processed as described above, and the signal

and noise spectra were overlain and visually inspected. A minimum and maximum frequency defining an acceptable contiguous band with a signal-to-noise ratio exceeding 3 was determined for each  $S$ -wave spectrum.

Figure 8 shows a composite plot of the 23 individual acceleration spectra as recorded and normalized to have equal amplitudes at 12 Hz. From Figure 8 it appears that these spectra have corner frequencies in the approximate range 15–25 Hz.

The regression model indicated by equation (8) was used to estimate  $\kappa_s$  at Lake Monticello, using the data shown in Figure 8. Estimates were also performed using the same data truncated at upper frequency values of 25, 20, and 15 Hz. The results are shown in Table 3 and indicate a systematic decrease in the estimate of  $\kappa_s$  as the truncation frequency of the data decreases. The values in Table 3 give an indication of estimation bias as a function of upper frequency limit for data sets composed of events with source corner frequencies in the 15–25 Hz range. For a corner frequency of 20 Hz and moment magnitude less than 0.6, the Brune (1970, 1971) model implies a stress drop of less than 1.0 bar for these very shallow, induced shocks.

#### Estimation of $\kappa_s$ in the Charleston Area

The Charleston area data are from substantially larger shocks compared to those studied at Lake Monticello. The average magnitude in Table 1 is 1.6, whereas the average magnitude for the Lake Monticello data set is 0.6. Additionally, the Charleston shocks are at midcrustal depths and are not associated with a reservoir. We would expect stress drops on the order of at least a few bars for these shocks. Corner frequencies in the range 15–25 Hz correspond to stress drops in the approximate range 1–10 bar for moment magnitude 1.6. On this basis, we view the Lake Monticello data as possibly representative of source spectra in the Charleston area, under a minimum stress drop condition. If corner frequencies are as low as 15–25 Hz in the Charleston area data set, we can expect that estimates of  $\kappa$  will be biased as indicated in Table 3.

The spectra of the  $S$  and  $Sp$  phases were calculated from transverse and vertical components, respectively. The two borehole stations RGR and CSB show distinct direct shear-wave arrivals and free surface reflections. A 0.25 sec processing window was used for the direct  $S$  arrival at RGR and CSB to isolate it from the reflection. Separation of the direct  $Sp$  arrival from the surface reflection is not feasible given the 100 sec<sup>-1</sup> sample rate of the data and shallow depths of the sensors. A 0.5 sec window was used for the  $Sp$  arrivals at all four stations. The  $S$  surface reflection at the borehole stations was also processed using a 0.5 sec window.

A total of  $n = 46$   $S$ ,  $Sp$ , and  $S/Sp$  spectra were obtained from the 25 earthquakes. Figure 9 shows  $S$  and  $Sp$  acceleration spectra from station CSB. Regressions using the model represented by equation (8) used data from all four stations to reduce potential bias from shallow, site-specific velocity variations. Because potential bias from this source is largely

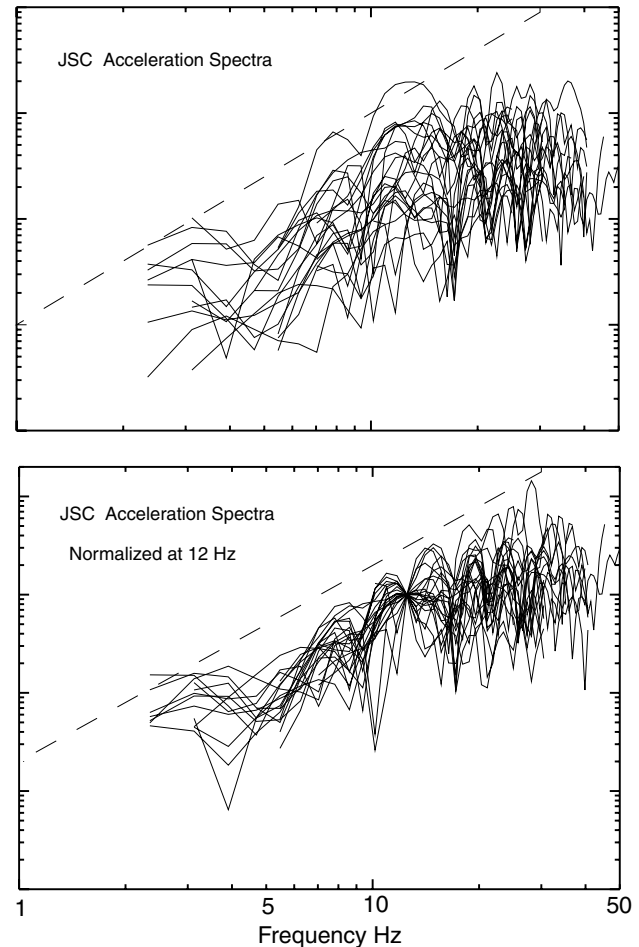


Figure 8. Top: relative acceleration spectra from the 23 earthquakes recorded at station JSC near Lake Monticello. Bottom: JSC acceleration spectra normalized to have equal amplitudes at 12 Hz. The dashed lines indicate an  $f^2$  spectral slope.

Table 3  
 $\kappa_s$  Estimates at Station JSC near Lake Monticello

Upper Frequency Limit	$\kappa_s$	Standard Error of Estimate
None	0.018	0.001
25 Hz	0.014	0.001
20 Hz	0.011	0.002
15 Hz	-0.004	0.003

due to spectral peaks at frequencies less than 10 Hz in this data set, the regressions were also performed using a narrow frequency band of 10–25 Hz.

Table 4 lists the results of this analysis. Figures 10, 11 and 12 show the residuals from the regressions using the  $S$  and  $Sp$  phases and the  $S/Sp$  ratio.

Figure 10 shows that the direct  $S$ -wave residuals for the borehole stations (CSB and RGR) are well fitted by the model in the sense that the residuals appear about equally distributed about zero throughout the entire frequency band. The

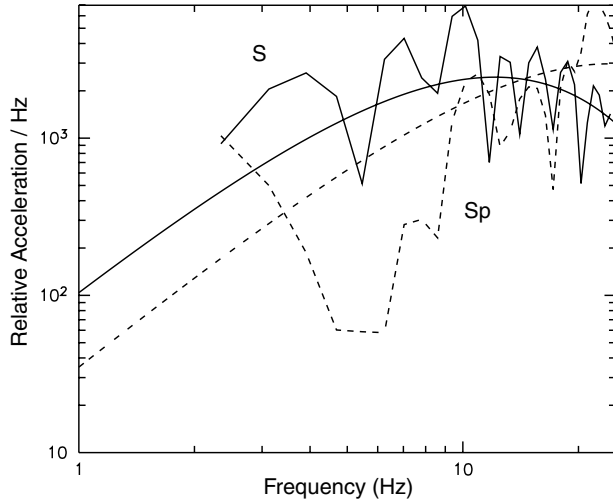


Figure 9. Acceleration amplitude spectra of  $S$  and  $Sp$  arrivals at CSB for the  $M = 2.0$ , 19 October 2000 earthquake. The smooth lines show the regression model fit to these data in the frequency range 10–25 Hz.

Table 4

Results of Regression Analysis of Data from the Charleston Area

Frequency Range (Hz)	$\kappa_s$	$\kappa_p$	$\kappa_s - \kappa_p$
0–30	$0.049 \pm 0.001$	$0.024 \pm 0.001$	$0.028 \pm 0.002$
10–25	$0.052 \pm 0.002$	$0.027 \pm 0.002$	$0.025 \pm 0.002$

residual plots for surface stations CSU and WAS show the effects of coherent site response amplification at frequencies less than 10 Hz. The  $Sp$  residuals for WAS also show the effects of strong amplification at approximately 7 and 12 Hz (Fig. 11). The  $Sp$  residuals for RGR and CSB are also modulated, but this is due to the inclusion of the free surface reflection in the processing window. The minima in the  $Sp$  residual plots for CSB and RGR correspond to maxima in the  $S/Sp$  residual plots shown in Figure 12, where the  $Sp$  spectra appear in the denominator of the spectral ratio. Although the presence of the  $P$ -wave free surface reflection is clearly a source of nonnormal residual behavior, it is not necessarily a strong source of bias in the estimation of  $\kappa_p$  or  $\kappa_s - \kappa_p$ . To illustrate, we can represent the time series containing the upgoing direct arrival and the downgoing surface reflection as the convolution of a wavelet with the sum of two delta functions:

$$W(t) = U(t) * [\delta(t) + \delta(t - \tau)], \quad (9)$$

where  $U(t)$  represents the wavelet shape of the direct and reflected arrivals and  $\tau$  is the travel time from the borehole sensor to the surface and back. The modulus of the Fourier transform is

$$|W(f)| = |U(f)| [2 + 2 \cos(2\pi f\tau)]^{1/2} \quad (10)$$

The modulating function has a constant mean. If the bandwidth of one complete cycle of modulation,  $1/\tau$ , is sufficiently small compared to the bandwidth of  $U(f)$ , the modulation will not seriously bias our estimate of an assumed linear slope of the high-frequency log amplitude spectrum of the wavelet. In the case of RGR and CSB, we have nearly two complete cycles of modulation in the observed spectra. In principle, the data could be corrected for this effect before performing the regression, but judging from the residual plots it does not appear to be necessary.

The small standard errors of estimate for the regression results shown in Table 4 have little significance because the regression residuals display the nonnormal, frequency-dependent characteristics mentioned above. In spite of this behavior, the results of the analysis seem to be robust. The results using the data set over the entire available frequency range of approximately 3–30 Hz are virtually identical to the results obtained using the restricted frequency band of 10–25 Hz. This is because of the “smoothing” that occurs in the simultaneous regression of data from all four stations. Prominent spectral peaks and troughs occur at different frequencies at these stations and tend to average out in the regression. Also, the estimates of  $\kappa_s$  and  $\kappa_p$  from the direct regression of the  $S$  and  $Sp$  arrivals agree with the estimate from the  $S/Sp$  spectral ratios. This also suggests that the results are stable and that the unknown source spectra of the earthquakes do not overwhelmingly bias the estimates of  $\kappa$ .

An idea of the resolution of the regression analysis can be had from Figure 13. The figure shows the behavior of the root mean square (rms) residual of the joint regression as a function of fixed values of  $\kappa$ . Figure 13 indicates that the practical limit of resolution in the estimation of  $\kappa$  is approximately  $\pm 0.01$ .

## Discussion

Important constraints are provided by the  $P$ -wave one-way vertical travel time of 0.363 sec through 775 m of sediments observed on reflection profiles near the stations and the average time interval of 0.74 sec between  $Sp$  and  $S$  at the stations. This allows us to directly estimate the vertical travel time of  $S$  through the sedimentary section: 1.10 sec. If we view the sedimentary section as a homogenous layer, we can (for comparison with other studies) estimate “average”  $P$ - and  $S$ -wave quality factors,  $Q_p$  and  $Q_s$ , by dividing the  $\kappa$  estimates by the vertical travel times. Using  $\kappa_s = 0.049$  and  $\kappa_p = 0.024$ , we obtain  $Q_s = 22$  and  $Q_p = 15$ .

It is important to compare these estimates with others derived from earthquake body waves at depths to several hundreds of meters in similar geological settings. Abercrombie (1997) listed several studies in California using borehole data that indicate  $Q_p$  values less than 45 and  $Q_s$  values less than 40 at depths greater than 100 m. The studies include Malin *et al.* (1988) ( $Q_s = 9$ –11), Aster and Shearer (1991) ( $Q_p = 27$ ,  $Q_s = 26$ ), Archuleta *et al.* (1992) ( $Q_s = 12$ ),

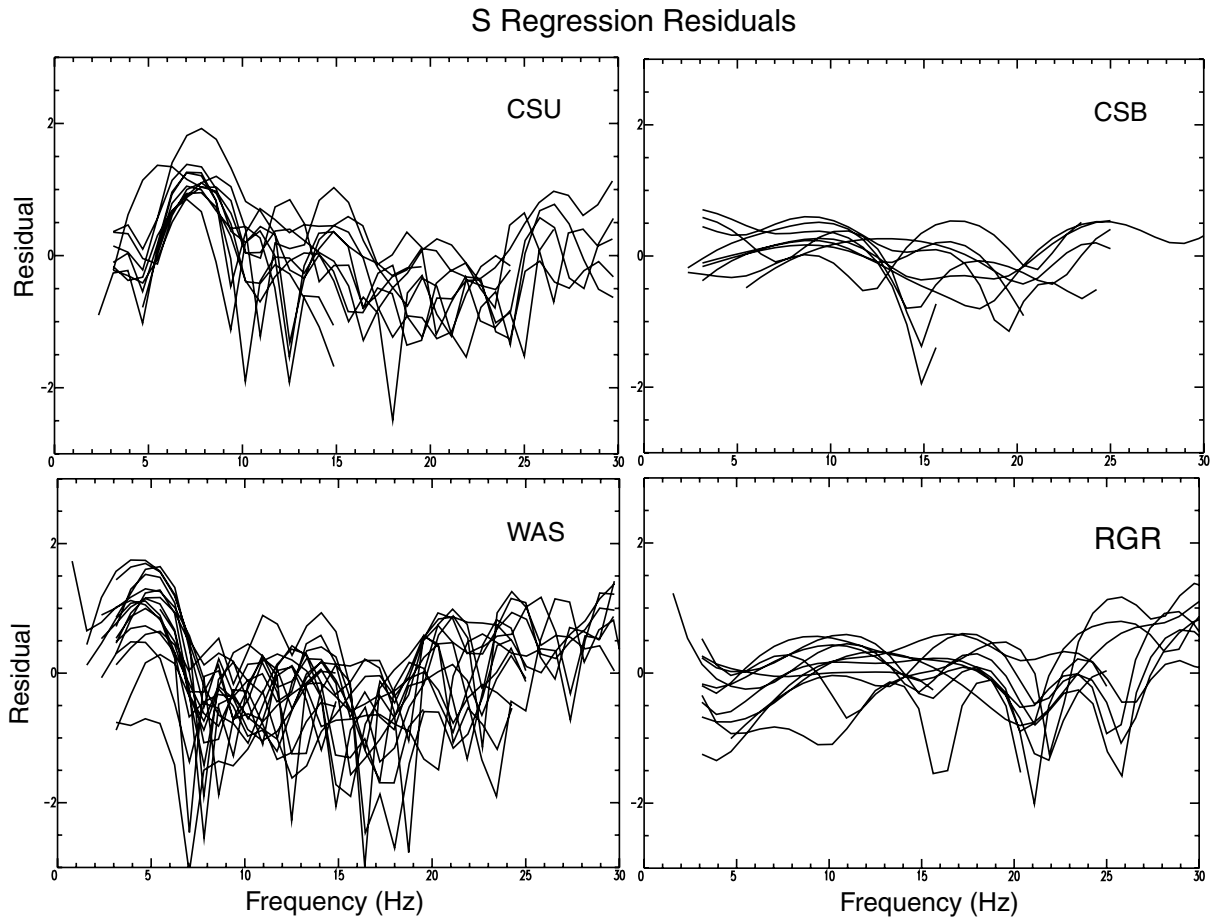


Figure 10. Residuals from the regression of the direct *S*-wave arrival at all stations. Surface stations CSU and WAS spectra use 0.5 sec windows. Stations CSB and RGR use 0.25 sec windows to isolate the direct *S* arrival from the free-surface reflection.

Gibbs *et al.* (1994) ( $Q_s = 15$ ), Blakeslee and Malin (1991) ( $Q_s = 8-19$ ,  $Q_p = 6-11$ ), Jongmans and Malin (1995) ( $Q_s = 10-37$ ), and Hauksson *et al.* (1987) ( $Q_s = 25$ ,  $Q_p = 44$ ). Abercrombie (1997) used a vertical array in the Cajon Pass Borehole to determine *P* and *S* spectral ratios at various depths, from 17 nearby earthquakes. A 300-m thick sedimentary section with *P* and *S* velocities of 1.79 and 0.657 km/sec, respectively, exhibited  $Q_s = 15$  and  $Q_p = 26$ .

The value of  $Q_s = 22$  appears typical of the work cited previously. However, the cited studies suggest that  $Q_p$  is approximately equal to or somewhat larger than  $Q_s$  at most locations where deep down hole measurements have been obtained. Both  $Q$  and velocity vary with depth within any thick sedimentary sequence. The estimates of “average”  $Q$  represent the integrated effects of attenuation over the entire depth range, represented by equation (3). Hence, the unexpected regression result  $Q_p < Q_s$  obtained in this study might be an indication of unusually low *P* velocity and/or  $Q_p$  at some depth in an otherwise typical sequence. The sonic log from cc1 does not show evidence of unusually low *P*-wave velocities at depth. However, the shallowest part of the sequence is not sampled well.

#### Near-Surface Velocities and Attenuation

The reflected phases on the borehole stations RGR and CSB provide information on the average velocities and attenuation to depths of 62 and 83 m at the respective sites. The average arrival-time interval between the upgoing *P* wave and the downgoing surface *P* reflection at RGR is  $0.07 \pm 0.01$  sec, determined in the time domain with accuracy limited by the 0.01 sec sample interval. Using this estimate, equation (10) predicts a spectral peak at approximately 14 Hz, as is observed in the residual plot shown in Figure 11. Another estimate of the *P*-wave reflection two-way time at RGR is possible by noting the prominent 8.5 Hz spectral null in Figure 11. This amplitude minimum indicates  $\tau = 0.059$  sec, from equation (10), and is the preferred estimate, leading to an estimate of average *P*-wave velocity in the upper 62 m at RGR of 2102 m/sec. At CSB, the observed interval between *P* and reflected *P* is 0.090 sec, and the average *P* velocity is 1844 m/sec. The average time intervals between direct *S* and the surface reflected *S* are 0.22 and 0.31 sec at RGR and CSB, respectively, giving 564 and 535 m/sec. The *P/S* velocity ratios from these estimates are 3.7 for RGR and

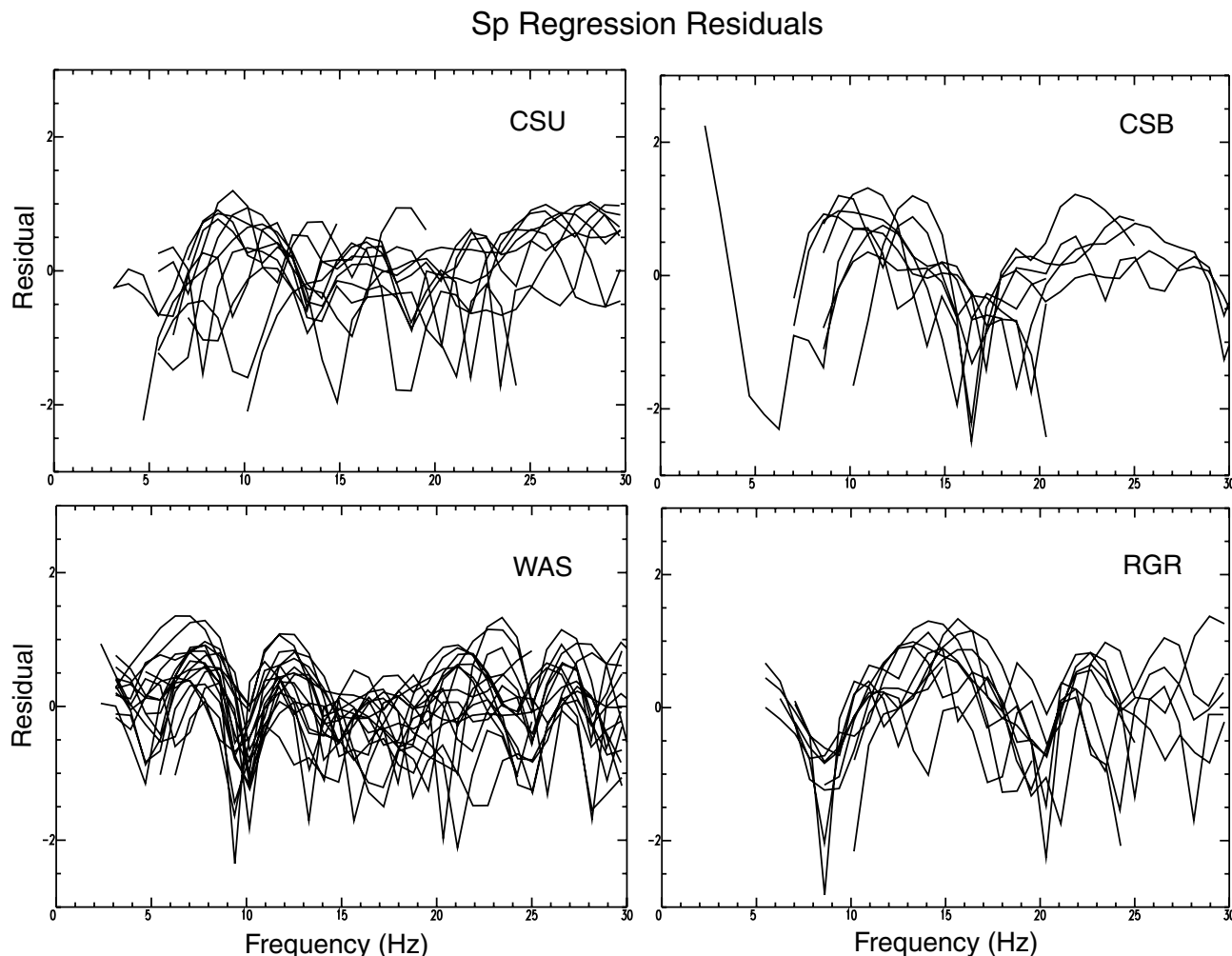


Figure 11. Residuals from the regression of the  $Sp$  wave packet at all stations. All stations use a 0.5 sec window, which includes both the direct and reflected  $Sp$  arrival at RGR and CSB.

3.4 for CSB. For comparison, Williams *et al.* (2000) found an average  $S$  velocity of 464 m/sec for the upper 30 m from shallow refraction profiling near New Hope, South Carolina, approximately 20 km to the north of RGR.

The average  $P$ -wave velocities at RGR and CSB over the sensor depth intervals are not much less than the observed average value of 2138 m/sec based on the known thickness of the entire sedimentary section at cc1 and the observed basement reflection travel time. On the other hand, the  $S$ -wave velocities are significantly less than the average value of 705 m/sec for the entire sequence, probably due to shear-wave velocities as low as 200 m/sec in the weathered zone within a few meters of the surface (Williams *et al.*, 2000). Therefore, we conclude that an anomalously low  $P$  velocity, or low  $P/S$  velocity ratio, does not exist at shallow depths at these sites. This cannot be the explanation for the low estimate of  $Q_p$  compared to  $Q_s$ .

It was not possible to derive estimates of  $Q_p$  from the direct  $P$  and reflected phases due to low signal-to-noise ra-

tios and overlapping arrivals. An unsuccessful attempt was made to estimate  $Q_s$  over the sensor depth intervals at RGR and CSB, using the direct and reflected  $S$  waves which are separated in time. In principle, the slope of the log ratio versus frequency function can give an estimate of  $-\pi\tau/Q_s$ , where  $\tau$  is the shear-wave travel time from sensor to surface and back. As shown in Figure 14, the spectral ratios are irregular, exhibiting large modulations, and slopes on the order of that expected for  $Q_s = 22$  cannot be resolved.

#### Potential Bias Due to Unknown Source Spectral Corner Frequencies

The analysis of the Lake Monticello data indicates the degree of bias to be expected in the estimates of  $\kappa_s$  if source corner frequencies are in the range 15–25 Hz. It is interesting to speculate on the effect this would have if it applied to the Charleston area data as well.

Let us assume that our estimates of  $\kappa_s$  for the Charleston area are  $0.014 \text{ sec}^{-1}$  too large, as suggested by the results

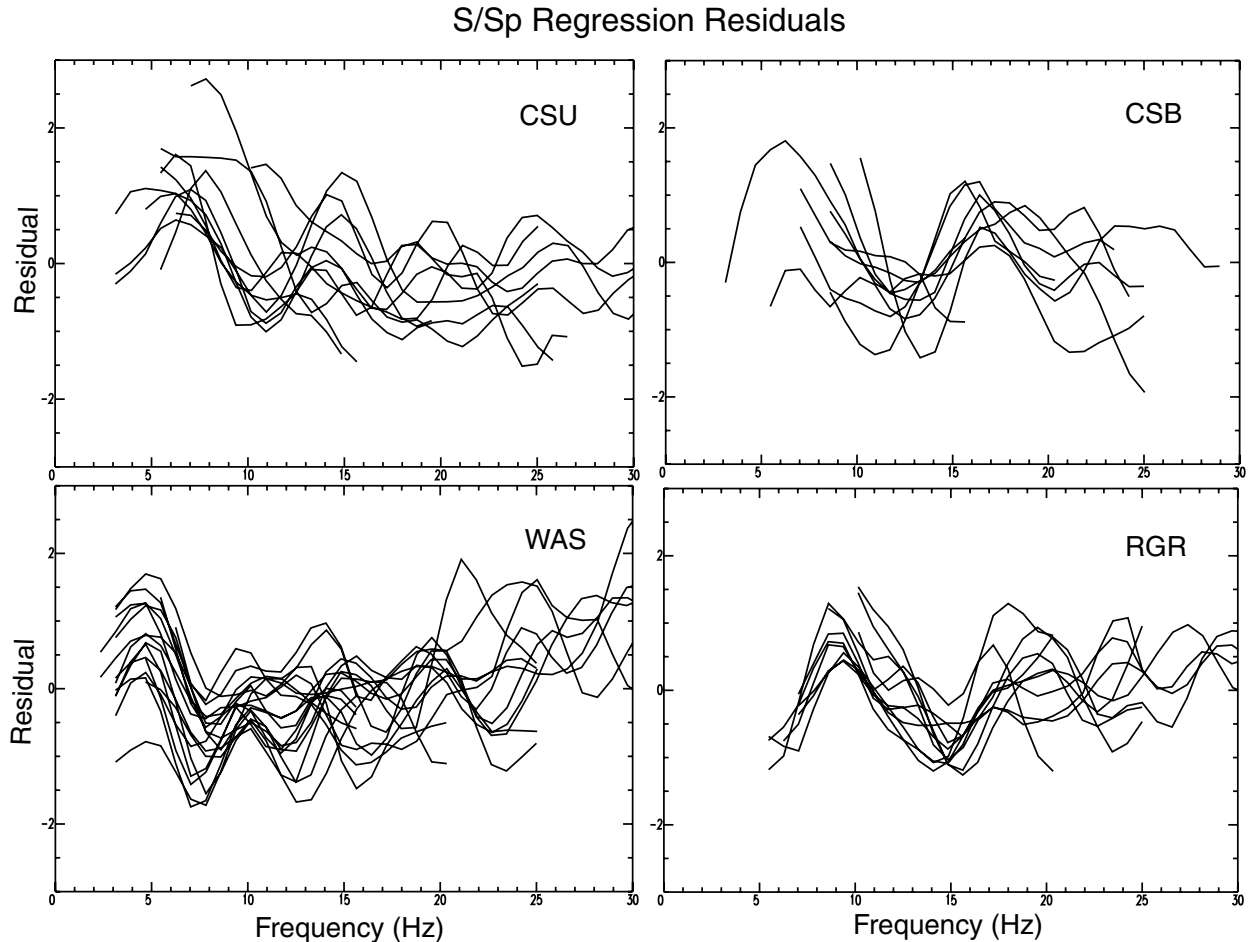


Figure 12. Residuals from the regression of the  $S/Sp$  ratio at all stations. All ratio spectra are based on 0.5 sec time windows, including both direct waves and reflections from the free surface at stations RGR and CSB.

shown in Table 3 for Lake Monticello, which are based on regression analysis of spectra over a frequency band to 25 Hz. In principle, the same bias would apply to our estimates of  $\kappa_p$  as well. Our estimates for  $\kappa_s - \kappa_p$  should be unbiased, due to cancellation of source terms in the  $S/Sp$  spectral ratio. In these circumstances, the unbiased values for  $\kappa_s$  and  $\kappa_p$  are 0.035 and 0.010, respectively. The corresponding “unbiased” estimates for  $Q_s$  and  $Q_p$  are 32 and 36, respectively. These numbers are consistent with most previous studies using vertical array data that find  $Q_p$  slightly greater than or equal to  $Q_s$ .

#### Implications for Ground-Motion Prediction

The geological conditions present in the Charleston area differ substantially from average conditions in the seismically active areas of western North America. Also, these conditions are not encountered in eastern North America outside the Gulf and Atlantic coastal margins and the Mississippi Embayment. Near Charleston, approximately 800–1000 m of unconsolidated sediment overlies Mesozoic sedimentary and volcanic rocks with shear-wave velocities in

excess of 3 km/sec. This velocity discontinuity is responsible for the observed  $Sp$  phases on the seismograms and can be expected to substantially modify the ground motion. Our results indicating  $\kappa_s$  in the range 0.035–0.049 suggest that high-frequency attenuation will be appreciable.

Figure 15 shows three site response functions based on a generalized velocity structure for Tertiary and Cretaceous units in the Charleston area. The response calculations assume  $\kappa_s$  values of 0.01, 0.049, and 0.035. Plotted are ratios defined by dividing the Fourier amplitude spectra of surface motion on a layered sediment section by the amplitude spectrum of surface motion on an outcrop of the basement. Vertically incident  $SH$  motion is assumed. The velocity structure consists of eight layers over a basement half-space and is shown in Figure 4. The calculations do not include the effects of the shallowest material in the Charleston area, consisting of Quaternary sands and clays with shear-wave velocities in the range 100–400 m/sec; these materials typically extend to depths of approximately 20 m. The response was calculated using the quarter-wavelength approximation of Boore and Joyner (1991), which produces a smoothed ver-

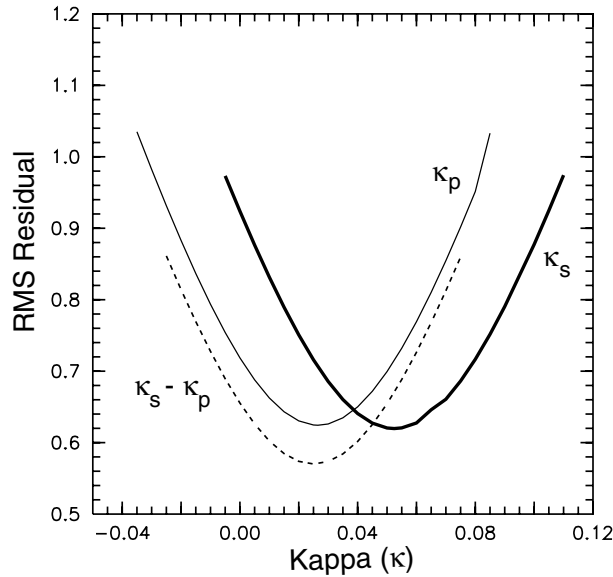


Figure 13. The rms residual versus  $\kappa$  for regression of data from near Charleston, South Carolina. The minimum value of the rms residual corresponds to the least-squares estimate of  $\kappa$ . The resolution of the regression is implied by the sharpness of the rms residual minima.

sion of the modulated transfer function for the layered structure. Shown for comparison with typical soil sites in eastern North America is the site response function developed for generic firm soil site conditions in the eastern United States for the 1996 National Seismic Hazard Mapping Project (Frankel *et al.*, 1996). The generic response function is based on  $\kappa_s = 0.01$ , assuming a velocity structure consisting of a steep gradient from the surface to approximately 200 m depth (650 to 2.25 km/sec) and a very gradual increase from 200 m to 8 km (2.25 to 3.6 km/sec). Velocities in the uppermost 30 m of the two models are comparable, but the shear-wave velocity remains less than 1000 m/sec to depths of approximately 800 m in the Charleston area. The response for the Charleston area derived here exceeds the generic B-C boundary response in the frequency range 0.2–1 Hz by as much as a factor of 1.8, due to the basement-sediment velocity discontinuity and greater thickness of the sediment section. The responses rapidly diverge at frequencies greater than 2 Hz due to inferred differences in attenuation, such that at 10 Hz, the amplification estimated for Charleston is only 0.5 (for  $\kappa_s = 0.035$ ) to 0.3 (for  $\kappa_s = 0.049$ ) of the generic B-C boundary response. This impacts predictions of high-frequency oscillator response and peak ground acceleration, as the larger values of  $\kappa_s$  reduce the bandwidth of the acceleration spectrum. Point source simulations of  $M = 7.0$  shocks using the stochastic model with  $\omega^2$  source spectra indicate reductions of peak accelerations by factors from 0.55 to 0.45 for  $\kappa_s$  in the range 0.035–0.049, compared to calculations using  $\kappa_s = 0.01$ .

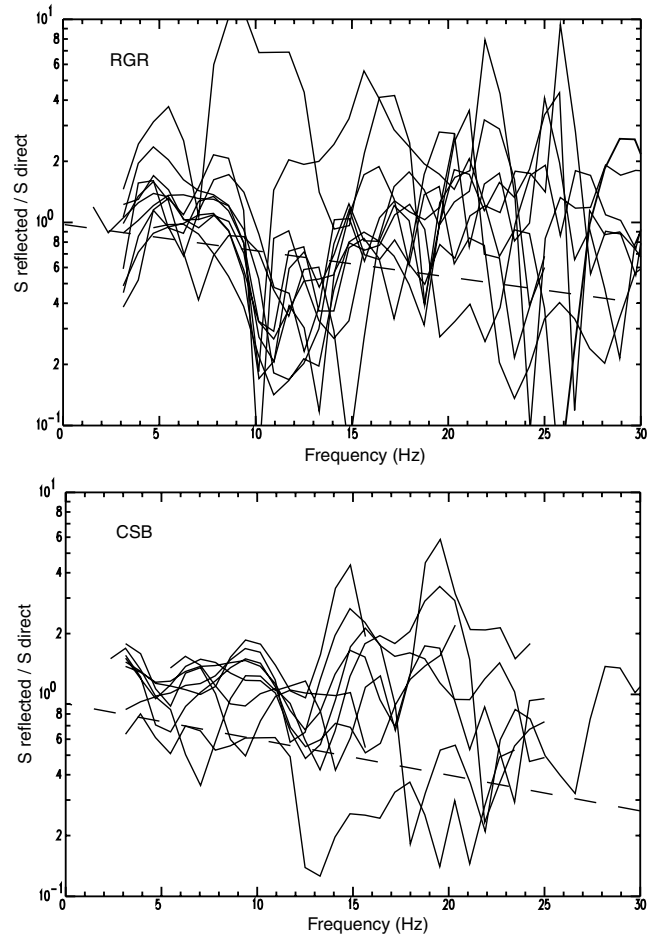


Figure 14. Spectral ratios of the surface reflected  $S$  arrival and the direct  $S$  wave at station RGR (top) and CSB (bottom). The dashed lines indicate the expected trends of the spectral ratios for  $Q_s = 22$ .

## Conclusions

Spectral analysis of direct  $S$  and  $S_p$  converted phases from nearby microearthquakes in the Atlantic Coastal Plain near Charleston, South Carolina, gives estimates of  $\kappa_s$  and  $\kappa_p$  of 0.049 and 0.024, respectively. These values should be viewed as upper-bound estimates because they are based on an untested assumption that the source spectral corner frequencies lie above the frequency band of the analysis, in excess of 25 Hz. The estimates would be biased upward if in fact the corner frequencies are smaller. The value of  $\kappa_s - \kappa_p$  derived from the direct  $S$  and  $S_p$  phases is equivalent to that derived from the regression of the spectral ratio, suggesting an absence of bias. However, bias of approximately  $0.015 \text{ sec}^{-1}$  or less cannot be ruled out due to limited resolution of the regression of the spectral ratio data. A similar analysis of reservoir-induced microearthquakes at Lake Monticello, South Carolina, in a high-velocity, hard-rock environment indicates a potential bias of  $0.014 \text{ sec}^{-1}$  from analysis of data to frequencies of 25 Hz, because the shallow,

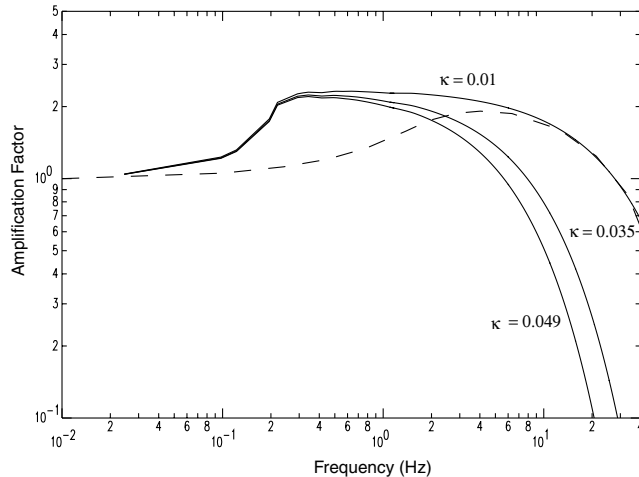


Figure 15. Solid lines show site response amplification (soil surface/basement outcrop) for three values of  $\kappa_s$ , using the shear-wave velocity profile shown in Figure 4 and assuming a constant density of 2000 kg/m<sup>3</sup> in the sedimentary section. The dashed line is a generic B-C boundary site response, taken from data in table A5 of Frankel *et al.* (1996).

induced shocks exhibit apparent corner frequencies in the 15–25 Hz band. Correcting the above values with that estimate of bias gives values of  $\kappa_s = 0.035$  and  $\kappa_p = 0.010$ .

These estimates of  $\kappa$  apply to the Middleton Place–Summerville seismic zone, which is approximately 30 km to the northwest of Charleston, South Carolina. The sedimentary section in that area is approximately 775 m thick, and average velocities for the vertical propagation of  $P$  and  $S$  waves are 2.14 and 0.70 km/sec, respectively. We favor the lower, bias-corrected estimates of  $\kappa$  because they imply nearly equivalent path-averaged estimates of  $P$  and  $S$  quality factors ( $Q_s = 32$ ,  $Q_p = 36$ ), whereas the uncorrected estimates of  $\kappa$  imply that  $Q_s$  is significantly larger than  $Q_p$  over some part of the path through the sedimentary section. This is considered unlikely on the basis of  $P$ - and  $S$ -wave velocity estimates at shallow depths derived from the times of direct and surface reflected waves at the two borehole station locations.

### Acknowledgments

This research was supported by the U.S. Geological Survey (USGS), Department of the Interior, under USGS Award Number 00HQGR0036. Reviews by Søren Gregersen, Arthur McGarr, and an anonymous referee improved the study. The views and conclusions contained in this article are those of the authors and should not be interpreted as necessarily representing the official policies, either expressed or implied, of the U.S. government.

### References

Abercrombie, R. A. (1997). Near-surface attenuation and site effects from comparison of surface and deep borehole recordings, *Bull. Seism. Soc. Am.* **87**, 731–744.

- Ackerman, H. D. (1983). Seismic-refraction study in the area of the Charleston, South Carolina, 1886 earthquake, *U.S. Geological Survey Profess. Pap.* 1313-F, 19 pp.
- Anderson, J. G., and S. E. Hough (1984). A model for the shape of the Fourier amplitude spectrum of acceleration at high frequencies, *Bull. Seism. Soc. Am.* **74**, 1969–1993.
- Archuleta, R. J., S. H. Seale, P. V. Sangas, L. M. Baker, and S. T. Swain (1992). Garner Valley downhole array of accelerometers: instrumentation and preliminary data analysis, *Bull. Seism. Soc. Am.* **82**, 1592–1621.
- Aster, R. C., and P. M. Shearer (1991). High-frequency borehole seismograms recorded in the San Jacinto fault zone, southern California. II. Attenuation and site effects, *Bull. Seism. Soc. Am.* **81**, 1081–1100.
- Benz, H. M., A. Frankel, and D. M. Boore (1997). Regional  $L_g$  attenuation for the continental United States, *Bull. Seism. Soc. Am.* **87**, 606–619.
- Blakeslee, S., and P. Malin (1991). High-frequency site effects at two Parkfield downhole and surface stations, *Bull. Seism. Soc. Am.* **81**, 332–345.
- Boore, D. M., and W. B. Joyner (1991). Estimation of ground motion at deep-soil sites in eastern North America, *Bull. Seism. Soc. Am.* **81**, 2167–2185.
- Brune, J. N. (1970). Tectonic stress and the spectra of seismic shear waves from earthquakes, *J. Geophys. Res.* **75**, 4997–5009.
- Brune, J. N. (1971). Correction, *J. Geophys. Res.* **76**, 5002.
- Chapman, M. C., and M. J. B. Rogers (1989). Coda  $Q$  in the southern Appalachians, *Geophys. Res. Lett.* **16**, no. 6, 531–534.
- Chen, K.-C., J.-M. Chiu, and Y.-T. Yang (1994).  $Q_p$ - $Q_s$  relations in the sedimentary basin of the upper Mississippi Embayment using converted phases, *Bull. Seism. Soc. Am.* **84**, 1861–1868.
- Chen, L., and P. Talwani (2001). Renewed seismicity near Monticello Reservoir, South Carolina, 1996–1999, *Bull. Seism. Soc. Am.* **91**, 94–101.
- Clouser, R. H., and C. A. Langston (1991).  $Q_p$ - $Q_s$  relations in a sedimentary basin using converted phases, *Bull. Seism. Soc. Am.* **81**, 733–750.
- Dutton, C. E. (1889). The Charleston earthquake of August 31, 1886, in *Ninth Annual Report of the U.S. Geol. Surv.* 203–528.
- Fletcher, J. B. (1995). Source parameters and crustal  $Q$  for four earthquakes in South Carolina, *Seism. Res. Lett.* **66**, no. 4, 44–58.
- Frankel, A. D., C. Mueller, T. Barnhard, D. Perkins, E. V. Leyendecker, N. Dickman, S. Hanson, and M. Hopper (1996). National Seismic-Hazard Maps: Documentation June 1996, *U.S. Geol. Surv. Open-File Rept.* 96-532, 71 pp.
- Frankel, A. D., M. D. Petersen, C. S. Mueller, K. M. Haller, R. L. Wheeler, E. V. Leyendecker, R. L. Wesson, S. C. Harmsen, C. H. Cramer, D. M. Perkins, and K. S. Rukstales (2002). Documentation for the 2002 update of the National Seismic Hazard Maps, *U.S. Geol. Surv. Open-File Rept.* 02-420, 33 pp.
- Garner, J. T. (1998). Re-evaluation of the seismotectonics of the Charleston, South Carolina area, *Master's Thesis*, University of South Carolina, Columbia.
- Gibbs, J. F., D. M., Boore, W. B. Joyner, and T. E. Fumal (1994). The attenuation of seismic shear waves in Quaternary alluvium in Santa Clara valley, California, *Bull. Seism. Soc. Am.* **84**, 76–90.
- Gohn, G. S. (1983). Studies related to the Charleston, South Carolina, earthquake of 1886: tectonics and seismicity, *U.S. Geol. Profess. Pap.* 1313.
- Hauksson, E., T.-L. Teng, and T. L. Henley (1987). Results from a 1500 m deep, three-level downhole seismometer array: site response, low  $Q$  values, and  $f_{max}$ , *Bull. Seism. Soc. Am.* **77**, no. 6, 1883–1904.
- Johnston, A. C. (1996). Seismic moment assessment of earthquakes in stable continental regions. III. New Madrid 1811–1812, Charleston, 1886, and Lisbon, 1755, *Geophys. J. Int.* **126**, 314–344.
- Jongmans, D., and P. E. Malin (1995). Vertical profiling of microearthquake  $S$  waves in the Varian well at Parkfield, California, *Bull. Seism. Soc. Am.* **85**, 1805–1820.
- Madabhushi, S., and P. Talwani (1993). Fault plane solutions and relocations of recent earthquakes in the Middleton Place–Summerville seis-

- mic zone near Charleston, South Carolina, *Bull. Seism. Soc. Am.* **83**, no. 5, 1442–1466.
- Malin, P. E., J. A. Waller, R. D. Borchardt, E. Cranswick, E. G. Jensen, and J. Van Schaack (1988). Vertical seismic profiling of Oroville microearthquakes: velocity spectra and particle motion as a function of depth, *Bull. Seism. Soc. Am.* **78**, 401–420.
- Rankin, D. W. (1977). Studies related to the Charleston, South Carolina, earthquake of 1886: a preliminary report, *U.S. Geol. Surv. Profess. Pap.* 1028.
- Rhea, S. (1984).  $Q$  determined from local earthquakes in the South Carolina Coastal Plain, *Bull. Seism. Soc. Am.* **74**, 2257–2268.
- Talwani, P. (1982). An internally consistent pattern of seismicity near Charleston, South Carolina, *Geology* **10**, 655–658.
- Talwani, P. (1999). Fault geometry and earthquakes in continental interiors, *Tectonophysics* **305**, 371–379.
- Talwani, P., and W. T. Schaeffer (2001). Recurrence rates of large earthquakes in the South Carolina Coastal Plain based on paleoliquefaction data, *J. Geophys. Res.* **106** (B4), 6621–6642.
- Williams, R. A., J. K. Odum, W. J. Stephenson, and D. M. Worley (2000). Determination of surficial  $S$ -wave seismic velocities of primary geological formations on the Piedmont and Atlantic Coastal Plain of South Carolina, Appendix A in *Site Response in the Atlantic and Gulf of Mexico Coastal Plains and Mississippi Embayment*, C. Mueller (Editor), U.S. Nuclear Reg. Comm./U.S. Geol. Surv. Interagency Agreement RES-99-002, report to NRC, April 10, 2000, pp. A1–A5.
- Yantis, B. R., J. K. Costain, and H. D. Ackerman (1983). A reflection seismic study near Charleston, South Carolina, *U.S. Geol. Surv. Profess. Pap.* 1313-G, 20 pp.

Department of Geological Sciences  
4044 Derring Hall  
Virginia Polytechnic Institute and State University  
Blacksburg, Virginia 24061  
mcc@vt.edu  
(M.C.C.)

Department of Geological Sciences  
University of South Carolina  
701 Sumter St.  
Columbia, South Carolina 29208  
talwani@geol.seis.sc.edu, cannon@geol.seis.sc.edu  
(P.T., R.C.C.)

Manuscript received 26 February 2002.